Combinatorial study of Ni–Ti–Pt ternary metal gate electrodes on HfO_2 for the advanced gate stack

K.-S. Chang,[a] M. L. Green, J. Suehle, E. M. Vogel, and H. Xiong
National Institute of Standards and Technology (NIST), Gaithersburg, Maryland 20899

J. Hattrick-Simpers, I. Takeuchi, and O. Famodu
Department of Materials Science and Engineering, University of Maryland, College Park, Maryland 20742

K. Ohmori, P. Ahmet, and T. Chikyow
National Institute of Materials Science (NIMS), Tsukuba 305-0044, Japan

P. Majhi, B.-H. Lee, and M. Gardner
Sematech, Austin, Texas 78741

(Received 14 April 2006; accepted 11 August 2006; published online 4 October 2006)

The authors have fabricated combinatorial Ni–Ti–Pt ternary metal gate thin film libraries on HfO_2 using magnetron co-sputtering to investigate flatband voltage shift (ΔV_{fb}), work function (Φ_m), and leakage current density (J_L) variations. A more negative ΔV_{fb} is observed close to the Ti-rich corner than at the Ni- and Pt-rich corners, implying smaller Φ_m near the Ti-rich corners and higher Φ_m near the Ni- and Pt-rich corners. In addition, measured J_L values can be explained consistently with the observed Φ_m variations. Combinatorial methodologies prove to be useful in surveying the large compositional space of ternary alloy metal gate electrode systems. © *2006 American Institute of Physics*. [DOI: 10.1063/1.2357011]

Due to aggressive demands to increase device performance, the traditional gate stack, SiO_2 gate dielectric, and polycrystalline Si gate electrode need to be replaced due to high leakage current density (J_L), polycrystalline Si depletion, and dopant diffusion effects.[1–3] The International Technology Roadmap for Semiconductors dictates that a 0.8 nm equivalent oxide thickness (EOT) gate dielectric is required for the 50 nm technology node in 2009.[4] In the past five years, high-k gate dielectrics have been studied extensively, and many potential materials such as HfO_2, ZrO_2, and their silicates and oxynitrides have shown promise as replacements for SiO_2.[1,3,5] However, identification of the metal gate electrode to replace polycrystalline Si is not as advanced. Metal gates offer an advantage over polycrystalline Si due to their intrinsically higher conductivity. However, metal gate stack integration involves complex issues such as the work function (Φ_m), flatband voltage shift (ΔV_{fb}), oxide charge (Q_{ox}), and thermal stability of the gate stack with regard to crystallization, interdiffusion, and interfacial reactions.[3,6] Elemental metal gates, even with appropriate Φ_m, may suffer adhesion and thermal stability problems.[7] Alloy metal gates might be a better solution, since one can tailor the desirable properties. However, exploring metal gate electrode alloys is not trivial, since fabrication based on a one-composition-at-a-time approach is too time consuming to investigate even one of the many possible ternary alloy systems. Combinatorial methodology offers a viable approach, since it incorporates high throughput and rapid characterization in parallel, and a large number of samples may be characterized.[8,9] The goal of this research is to demonstrate the efficiency of combinatorial techniques to enable rapid exploration of the electrical and physical properties of the Ni–Ti–Pt ternary metal gate electrode system on HfO_2, through the deposition of a combinatorial ternary alloy "library." The strategy for choosing these three elements is their wide range of Φ_m in the bulk (Ni: 4.9 eV, Pt: 5.3 eV, and Ti: 4.1 eV).[10] Thus, in the ternary metal system, one can expect n-channel metal-oxide-silicon (NMOS) metals (4.05 ± 0.2 eV, aligned with the Si conduction band edge) and p-channel metal-oxide-silicon (PMOS) metals (5.17 ± 0.2 eV, aligned with the Si valence band edge). We systematically investigated ΔV_{fb}, Φ_m, and J_L, which offer a basis for understanding the gate stack properties, through capacitance-voltage (C-V) and current-voltage (I-V) analyses of Ni–Ti–Pt/HfO_2 capacitors.

Ni–Ti–Pt ternary libraries (composition spreads) were fabricated using an ultrahigh vacuum (base pressure of $\sim 10^{-9}$ torr) magnetron co-sputtering system.[11] Three sputtering guns were placed in a parallel, triangular configuration that allowed a natural compositional mix due to overlap of the three component metals [Fig. 1(a)]. The applied power for sputtering the Ni, Ti, and Pt targets was adjusted to optimize deposition rate. Each gun was housed in a 2 in. long chimney to minimize cross contamination. The libraries were deposited on Si wafers (p-type, resistivity of $\sim 0.02\ \Omega$-cm) predeposited with 6 nm of atomic layer deposited (ALD) HfO_2.[12] A Si shadow mask with hundreds of nominal ($250 \times 250\ \mu m^2$) openings was placed directly on top of the wafer to result in *in situ* metal-oxide-silicon capacitors (MOSCAPS). The thickness of the library films was ~ 50 nm; a thin layer of Pt (~ 5 nm) was uniformly deposited after the library deposition to minimize oxidation of the Ti-rich alloys. A forming gas annealing (90% N_2 and 10% H_2) was carried out at 500 °C for 30 min to lower the interface state density. Wavelength dispersive spectroscopy (WDS) and scanning x-ray microdiffraction were used to characterize the nominal compositions and structures of the library. An *LCR* meter with a parallel *RC* circuit mode and a precision semiconductor parameter analyzer were used to measure C and J_L, respectively. The modulation signal level was set at 50 mV for the C measurement, and C-V behavior

[a]Also at University of Maryland; electronic mail: kao-shuo.chang@nist.gov

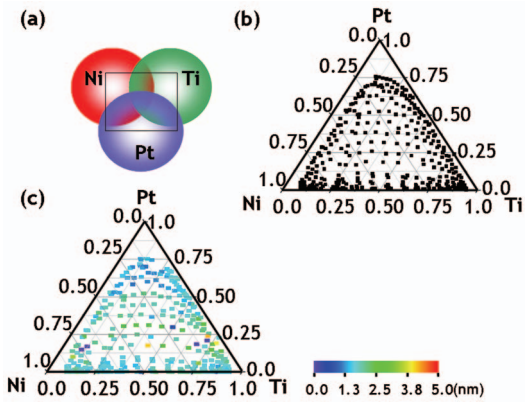

FIG. 1. (Color) (a) Schematic drawing of the configuration of the three component metals, Ni, Ti, and Pt, in the combinatorial magnetron co-sputtering system, (b) nominal composition map characterized by wavelength dispersive spectroscopy (WDS), and (c) extracted equivalent oxide thickness (EOT) across the Ni–Ti–Pt library. The mode of the EOT values is about 1.9 nm.

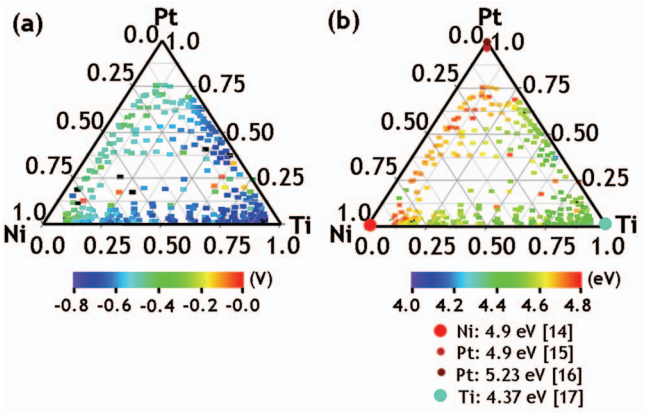

FIG. 2. (Color) (a) Map of the flatband voltage shift (ΔV_{fb}) extracted from the *C-V* characteristics at 1 kHz across the Ni–Ti–Pt libraries and (b) map of the extracted work functions (Φ_m) across the library. Round symbols in the three corners denote literature values.

was measured at 1 kHz to avoid series resistance. The Si substrate was biased for both measurements to reduce the noise ratio. The *C-V* and *I-V* properties of hundreds of MOSCAPS were measured using an automatic probe. Statistically reliable J_L values were obtained by averaging ten consecutive measurements at an applied dc substrate bias of 1 V. A standard program[13] was used to fit the measured *C-V* curves, to extract EOT and ΔV_{fb}.

Figure 1(b) shows the composition map of the Ni–Ti–Pt library, characterized by WDS. A wide composition range, with over 90% ±1% atomic ratio of Ni and Ti and 75% ±1% atomic ratio of Pt, was achieved. The lower percentage of Pt resulted from an unintentionally low Pt deposition rate. The MOSCAP EOT values are plotted in Fig. 1(c). Some data points are missing, corresponding to bad devices that could not be fitted automatically. The mode of the EOT values is about 1.9 nm, greater than the nominal EOT value expected for 6 nm HfO_2 (corresponding to 1.2 nm, assuming a dielectric constant for HfO_2 of 20), due to the interfacial oxide layer between HfO_2 and the Si substrate, which was observed by transmission electron microscopy (not shown).

Scanning x-ray microdiffraction was used to study the structure of the Ni–Ti–Pt ternary alloys. Face centered cubic (FCC) polycrystalline structures were observed near the Pt- and Ni-rich corners, as expected, but no peaks were observed near the Ti-rich corner, indicating that a nanocrystalline structure is most likely present. Many intermetallic phases observed in the bulk Ni–Ti–Pt phase diagrams were not observed in our library film. This might suggest that few of the expected intermetallic compounds form in the thin film or their nanocrystalline structures cannot be observed by x-ray diffraction.

Φ_m of various metals can be approximated from the ΔV_{fb} data, extracted from *C-V* curves, using the following relationship:

$$\Delta V_{\mathrm{fb}} = (\Phi_m - \Phi_s) - (Q/C_{\mathrm{ox}}), \tag{1}$$

where Φ_m and Φ_s are the work functions of metal and Si, respectively, Q is the charge in HfO_2, and C_{ox} is the capacitance. Figure 2(a) shows the ΔV_{fb} map extracted from MOSCAPS across the Ni–Ti–Pt library. A systematic and smooth variation is observed across the library. The smooth variation of ΔV_{fb} suggests that many of the phases present in the bulk Ni–Ti–Pt alloy phase diagram are suppressed in the thin film. The ΔV_{fb} values close to the Ni- and Pt-rich corners are less negative (~−0.3 V) than at the Ti-rich corner (~−0.8 V). From Eq. (1) therefore, Φ_m near the Ni- and Pt-rich corners should be larger than at the Ti-rich corner. Assuming Q/C_{ox} is roughly constant as a function of metal gate composition, the variation in ΔV_{fb} is directly related to the change of Φ_m. Figure 2(b) shows the map of Φ_m variation across the library, derived from Fig. 2(a), using data generated by the CVC program. The trend is consistent with our expectation. The extracted values close to the three corners are comparable with literature values (round symbols) for Ni and Ti, but only with the low end of the literature values for Pt.[14–17] Thus, nowhere in the library do we observe an alloy with Φ_m suitable for PMOS. This might be interpreted in two ways: (1) only 75% Pt was achieved, which results in more negative ΔV_{fb} (smaller Φ_m) compared to 100% Pt or (2) some midgap states were created at the metal/HfO_2 interfaces, resulting in interface dipoles and Fermi-level pinning.[18] Currently, we are making library films with a new combinatorial technique, which will allow us to explore the complete ternary up to 100% of each corner element to further elucidate this issue.

In a metal/insulator/semiconductor structure,[19] metals with higher Φ_m intrinsically possess higher barrier height (ϕ_0) based on the equation

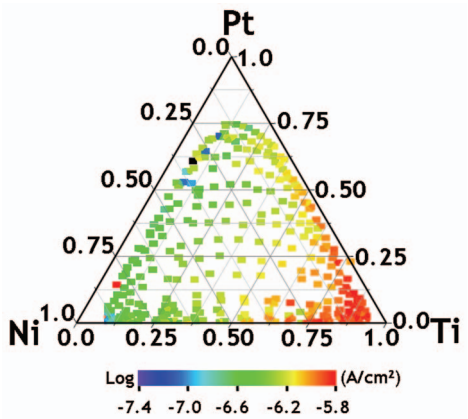

FIG. 3. (Color) Leakage current density (J_L) map measured at an applied dc substrate bias of 1 V.

$$\phi_0 = \Phi_m - \chi_i, \tag{2}$$

where χ_i is the insulator electron affinity, a constant. From the data of Fig. 2(b), Ni- and Pt-rich alloys, possessing higher Φ_m, should accordingly have higher ϕ_0, and Ti-rich alloys, possessing smaller Φ_m, smaller ϕ_0. The relationship between J_L and ϕ_0 is shown in the following equation:[19]

$$J_L \propto E^2 \exp\left(\frac{-8\pi\sqrt{2m^*}(q\phi_0)^{3/2}}{3qhE}\right), \tag{3}$$

where E is the electric field across the oxide, q is the charge of an electron, h is Planck's constant, and m^* is the effective mass of an electron in the oxide. One can see that higher ϕ_0 results in smaller J_L. Therefore, Ni- and Pt-rich alloys will result in smaller J_L, and Ti-rich alloys, higher J_L. Figure 3 shows a J_L map of the Ni–Ti–Pt library. We observe that the devices near the Ni- and Pt-rich corners have smaller J_L ($\log J_L \sim -7.4$ A/cm^2), gradually increasing towards the Ti-rich corner ($\log J_L \sim -5.8$ A/cm^2). This is consistent with our expectations, and the measured J_L values are comparable with literature values.[20] Thus, the results of Figs. 2 and 3 are consistent, and Φ_m and J_L vary predictably with compositions in the Ni–Ti–Pt library.

In conclusion, Ni–Ti–Pt ternary metal gate libraries were deposited on HfO_2 dielectrics, and studied systematically by WDS, x-ray microdiffraction, and *C-V* and *I-V* analyses. WDS results show that over $90\% \pm 1\%$ of Ni and Ti and $75\% \pm 1\%$ of Pt were attained in the library. The fitted *C-V* characteristics reveal that the mode of the EOT value is about 1.9 nm, larger than expected, due to interfacial oxide. A more negative ΔV_{fb} is observed close to the Ti-rich corner than close to the Ni- and Pt-rich corners, implying smaller Φ_m near the Ti-rich corners and higher Φ_m near Ni- and Pt-rich corners. Measured J_L values vary predictably and are consistent with the extracted Φ_m variations.

The authors would like to thank Chris Long for assistance with the x-ray diffraction analysis. This research was partly supported by Japan Society for the promotion of Science, Core to Core program.This work was preformed in part at the NIST Center for Nanoscale Science and Technology's Nanofab facility in Gaithensburg, MD.

[1] G. D. Wilk, R. M. Wallace, and J. M. Anthony, J. Appl. Phys. **89**, 5243 (2001).
[2] P. A. Packan, Science **285**, 2079 (1999).
[3] H.-S. P. Wong, IBM J. Res. Dev. **46**, 133 (2002).
[4] International Technology Roadmap for Semiconductors, 2003, http://public.itrs.net
[5] J. Okabayashi, S. Toyoda, H. Kumigashira, M. Oshima, K. Usuda, M. Niwa, and G. L. Liu, Appl. Phys. Lett. **85**, 5959 (2004).
[6] G. A. Brown, P. M. Zeitzoff, G. Bersuker, and H. R. Huff, Mater. Today **7**, 20 (2004).
[7] V. Misra, H. Zhong, and H. Lazar, IEEE Electron Device Lett. **23**, 354 (2002).
[8] X.-D. Xiang and P. G. Schultz, Physica C **283–287**, 428 (1997).
[9] X.-D. Xiang, X. Sun, G. Briceno, Y. Lou, K.-A. Wang, H. Chang, W. G. Wallace-Freedman, S.-W. Chen, and P. G. Schultz, Science **268**, 1738 (1995).
[10] S. O. Kasap, *Principles of Electronic Materials and Devices* (McGraw Hill, Columbus, OH, 2002).
[11] I. Takeuchi, O. O. Famodu, J. C. Read, M. A. Aronova, K.-S. Chang, C. Craciunescu, S. E. Lofland, M. Wuttig, F. C. Wellstood, L. Knauss, and A. Orozco, Nat. Mater. **2**, 180 (2003).
[12] M. L. Green, A. J. Allen, X. Li, J. Wang, J. Llavsky, A. Delabie, R. L. Puurunen, and B. Brijs, Appl. Phys. Lett. **88**, 032905 (2006).
[13] J. R. Hauser and K. Ahmed, *Characterization and Metrology for ULSI Technology* (AIP, Woodbury, NY, 1998), pp. 235–239.
[14] Q. Li, Y. F. Dong, S. J. Wang, J. W. Chai, A. C. H. Huan, Y. P. Feng, and C. K. Ong, Appl. Phys. Lett. **88**, 222102 (2006).
[15] J. K. Schaeffer, L. R. Fonseca, S. B. Samavedam, Y. Liang, P. J. Tobin, and B. E. White, Appl. Phys. Lett. **85**, 1826 (2004).
[16] Y.-C. Yeo, T.-J. King, and C. Hu, J. Appl. Phys. **92**, 7266 (2002).
[17] H. Yang, Y. Son, S. Baek, H. Hwang, H. Lim, and H.-S. Jung, Appl. Phys. Lett. **86**, 092107 (2005).
[18] H. Y. Yu, C. Ren, Y.-C. Yeo, J. F. Kang, X. P. Wang, H. H. H. Ma, M.-F. Li, D. S. H. Chan, and D.-L. Kwong, IEEE Electron Device Lett. **25**, 337 (2004).
[19] S. M. Sze, *Physics of Semiconductor Devices* (Wiley, Taipei, Taiwan, 1981), pp. 364 and 403.
[20] N.-J. Seong, S.-G. Yoon, S.-J. Yeom, H.-K. Wod, D.-S. Kil, J.-S. Roh, and H.-C. Sohn, Appl. Phys. Lett. **87**, 132903 (2005).